



Estimation of aboveground biomass of arboreal species in the semi-arid region of Brazil using SAR (synthetic aperture radar) images

Janisson B de JESUS¹, Tatiana M KUPLICH², Íkaro D de C BARRETO³,
Fernando L HILLEBRAND⁴, Cristiano N da ROSA⁵

¹ Postgraduate Program in Remote Sensing, Federal University of Rio Grande do Sul, Campus Vale, Porto Alegre 91501970, Brazil;

² National Institute for Space Research (INPE), COESU (Southern Spatial Coordination), Santa Maria 97105970, Brazil;

³ Postgraduate Program Biometry and Applied Statistics, Rural Federal University of Pernambuco, Recife 52171900, Brazil;

⁴ Federal Institute of Education, Science and Technology of Rio Grande do Sul (IFRS), Campus Rolante, Rolante 95690000, Brazil;

⁵ Postgraduate Program in Remote Sensing, Polar and Climate Center, Federal University of Rio Grande do Sul, Porto Alegre 91501970, Brazil

Abstract: The Caatinga biome is an important ecosystem in the semi-arid region of Brazil. It has significantly degraded due to human activities and is currently a region undergoing desertification. Thus, monitoring the variation in the Caatinga biome has become essential for its sustainable development. However, traditional methods for estimating aboveground biomass (AGB) are time-consuming and destructive. Remote sensing, such as optical and radar imaging, can estimate and correlate with vegetation. Nevertheless, radar imaging is still a novelty to be applied in estimating the AGB of this biome, which is an area with little research. Therefore, this study aimed to use Sentinel-1 images to estimate the AGB of the Caatinga biome in Sergipe State (northeastern Brazil) and to verify its influencing factors. Nineteen sample plots (30 m×30 m) were selected, and the stems of individuals with a circumference at breast height (1.3 m above the ground) equal to or greater than 6.0 cm were measured, and the AGB through an allometric equation was estimated. The Sentinel-1 images from 3 different periods (green, intermediate, and dry periods) were used to consider the phenological conditions of the Caatinga biome. All the pre-processing and extraction of attributes (co-polarized VV (vertical transmit and vertical receive), cross-polarized VH (vertical transmit and horizontal receive), and band ratio VH/VV backscatter, radar vegetation index, dual polarization synthetic aperture radar (SAR) vegetation index (DPSVI), entropy (H), and alpha angle (α)) were performed with Sentinel's Application Platform. These attributes were used to estimate the AGB through simple and multiple linear regressions and evaluated by the coefficients of determination (R^2), correlation (r), and root mean squared error (RMSE). The results showed that the attributes individually had little ability to estimate the AGB of the Caatinga biome in the three periods. Combined with multiple regression, we found that the intermediate period presented the equation with the best results among the observed and estimated variables ($R^2=0.73$; $r=0.85$; $RMSE=8.33$ Mg/hm²), followed by the greenness period ($R^2=0.72$; $r=0.85$; $RMSE=8.40$ Mg/hm²). The attributes contributing to these equations were VH/VV, DPSVI, H, α , and co-polarized VV for the green period and cross-polarized VH for the intermediate period. The study showed that the Sentinel-1 images could be used to estimate the AGB of the Caatinga biome in the green and intermediate phenological periods since the SAR attributes highly correlated with the estimated variable (i.e., AGB) through multiple linear equations.

*Corresponding author: Janisson B de JESUS (E-mail: janisson.eng@gmail.com)

Received 2022-11-04; revised 2023-04-12; accepted 2023-04-23

© Xinjiang Institute of Ecology and Geography, Chinese Academy of Sciences, Science Press and Springer-Verlag GmbH Germany, part of Springer Nature 2023

Keywords: Caatinga; tropical dry forest; coherent and incoherent attributes; C-band; Sentinel-1

Citation: Janisson B de JESUS, Tatiana M KUPLICH, Íkaro D de C BARRETO, Fernando L HILLEBRAND, Cristiano N da ROSA. 2023. Estimation of aboveground biomass of arboreal species in the semi-arid region of Brazil using SAR (synthetic aperture radar) images. *Journal of Arid Land*, 15(6): 695–709. <https://doi.org/10.1007/s40333-023-0017-4>

1 Introduction

Drylands are important ecosystems extending over 40% of the Earth's surface (Sørensen, 2007). Their different biomes cover two-fifths of the Earth, with the semi-arid domain being the largest among the aridity zone (Bastin, 2017). In South America, among the three extensions of the existing semi-arid land, the Caatinga biome stands out as being the representative of this climate zone in Brazil, which is characterized by high annual average temperatures, high spatial and temporal variability of precipitation, and strong evaporation (Nóbrega et al., 2016). According to the Brazilian Ministry of Environment (MMA, 2021), this biome occupies roughly 11% of the country's territory across ten states.

The ecological, social, and economic issues in this region are obstacles for the biome since the semi-arid land of Brazil is undergoing desertification, which is aggravated by deforestation and land abandonment due to activities such as agriculture, grazing, and energy use (use of firewood). These activities increase soil degradation and reduce precipitation, making the area more vulnerable to droughts (Althoff et al., 2016; Salvatierra et al., 2017; Vendruscolo et al., 2020). Given this issue, researchers have sought to shed more light on this process and its consequences in Brazil (Vieira et al., 2015; Tomasella et al., 2018; Bezerra et al., 2020; Vieira et al., 2020, 2021; Barbosa Neto et al., 2021).

As the area of the Caatinga biome has decreased, it is necessary to identify the quantity of its vegetation biomass and verify its loss. This is relevant knowledge for research on the contribution of this type of vegetation for releasing or storing carbon (Menezes et al., 2021). Evaluating AGB using field measurements is commonly used in the Caatinga biome, as recent studies have shown (Souza et al., 2019; Castanho et al., 2020a; Maia et al., 2020; Menezes et al., 2021; Oliveira et al., 2022).

Although AGB (aboveground biomass) measurements based on traditional methods (such as forest inventories) provide accurate results, these techniques are laborious and time-consuming. Therefore, it is crucial to develop new strategies that can help to estimate biomass indirectly, such as remote sensing (Baccini et al., 2004; Akhtar et al., 2020). Various remote sensors based on different characteristics are used to estimate the AGB of vegetation. The primary data sources are optical, LiDAR (light detection and ranging), and radar (Kumar et al., 2015).

In the Caatinga biome, despite only a handful of studies estimating the AGB through traditional methods in different vegetation types, there is still a lack of application of remote sensing techniques to estimate the AGB. There are some studies at the local level (Lima Júnior et al., 2014; Fernandes, 2018; Silveira et al., 2020; Oliveira et al., 2021) and at the global scale using optical orbital sensors and LiDAR (Saatchi et al., 2011; Baccini et al., 2012). Therefore, there is a lack of use of active synthetic aperture radar (SAR) sensors in this biome.

SAR imaging has specific advantages compared with optical imaging, mainly in the biomass estimation in regions with characteristics of savanna to which the Caatinga resembles. Some of them are that the longer the wavelength of microwaves, the fewer effects from the clouds, which is vital in tropical environments with nearly constant cloud cover; in addition, microwaves interact directly with the vegetation structure by being able to cross the canopy (Kumar et al., 2015). Sentinel-1, a newly functioning orbital radar launched by the European Space Agency (ESA), operates at the C-band wavelength and provides free imaging (Nuthammachot et al., 2022). Its data have been used in studies on estimating AGB in forests (Forkuor et al., 2020; Mayamanikandan et al., 2020; Safari and Sohrabi, 2020; Ghosh and Behera, 2021; Malhi et al., 2021; Vaghela et al., 2021).

Given the characteristics of Sentinel-1, one can assume that the data obtained from this radar

will allow a significant interaction with the biomass of the arboreal Caatinga biome, considering the penetration of the microwave pulse into the canopy and the interaction with the structural characteristics of this vegetation, mainly during the period of lower leaf cover. Therefore, this study sought to evaluate Sentinel-1 SAR C-band images to estimate the aerial biomass of the Caatinga biome in three different phenological periods of vegetation leaf cover (green, intermediate, and dry periods), verifying the period and attribute(s) that most correlate with AGB.

2 Materials and methods

2.1 Study area

This study was conducted near the Grota do Angico Natural Monument Conservation Unit in the municipalities of Canindé de São Francisco and Poço Redondo in Sergipe State (Fig. 1), a region in the semi-arid region of Brazil according to the National Institute of the Semi-arid (INSA, 2019). The local climate is classified as BSh (hot arid steppe climate) by the Köppen classification, with annual precipitation below 700 mm and an average temperature of 24°C–26°C (Alvares et al., 2014). This portion of the state has monthly aridity indices that lead to a high risk of desertification (Jesus et al., 2019a). It is considered as a desertification area by the National Forest Inventory of the Brazilian Forest Service (MMA, 2018).

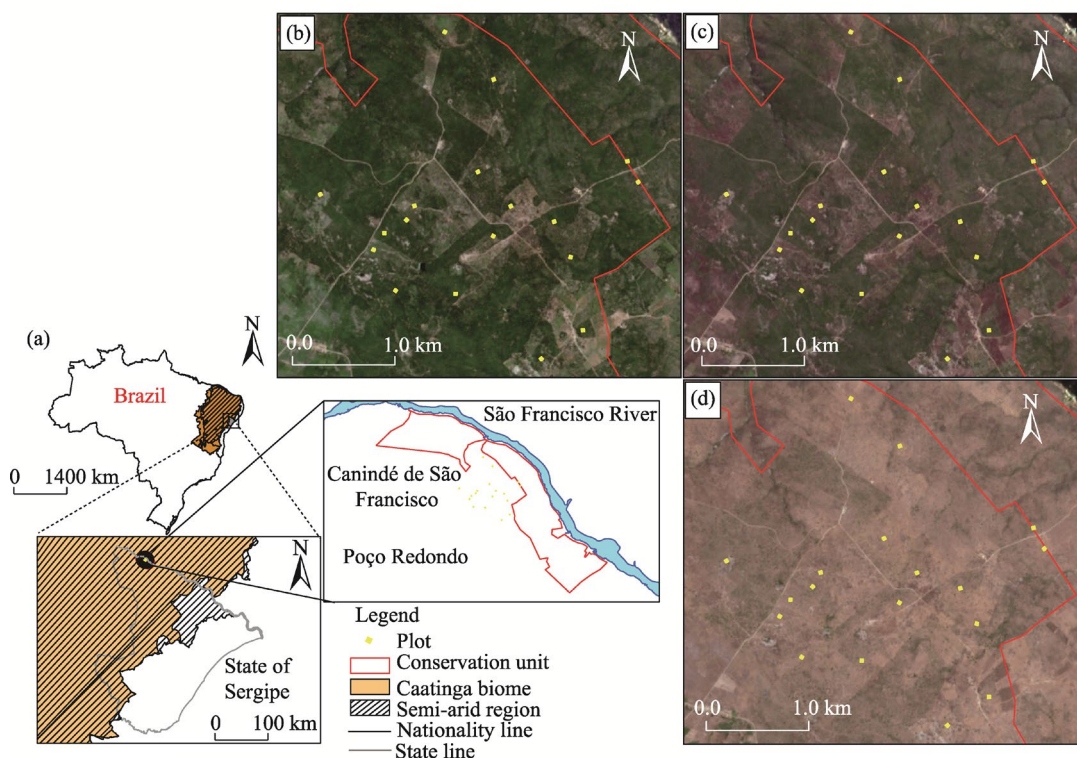


Fig. 1 Location of the study area and distribution of the sample plots (a). Variation in the leaf cover of the Caatinga Biome considering three phenological periods: green (b), intermediate (c), and dry (d) periods from Sentinel-2 images (RGB (red-green-blue): 4/3/2) dated 2018/12/27 (yyyy/mm/dd), 2019/09/28, and 2019/12/02, respectively (ESA, 2020a). The delimitation of the semi-arid region and the occurrence of the Caatinga biome in Brazil are also illustrated.

The vegetation is characteristic of the Caatinga biome and is composed of deciduous thorny trees and shrubs, which is typical of semi-arid to arid climates (Veloso et al., 1991), with dense forest remnants of hyper-xerophytic Caatinga (Ribeiro and Mello, 2007) occurring in different physiographic characteristics of the studied region (Jesus et al., 2019b). This plant typology has

high phenological variation in leaf cover due to varying rainfall supply (Jesus et al., 2021), and is categorized as a tropical dry forest (FAO, 2012). The soils are Luvisolos and Planossolos (Embrapa, 2011), with dissected reliefs on hills, tabular interflows, and a pediplan surface in the Sertão Pediplano (SEMARH, 2012).

2.2 Methodological flowchart

The study comprised two stages between field activity and analysis of Sentinel-1 images (Fig. 2). The first aimed to perform a forest inventory of arboreal Caatinga species to estimate biomass from densitometric calculations. Initially, a pilot inventory with six plots was performed to test the feasibility of applying the data collection method used and selecting all areas to implement the sample plots. Subsequently, 12 plots were measured to complete the inventory. The second stage of the study was related to acquiring and pre-processing the Sentinel-1 images, concluding with generating and extracting attributes in each respective sample unit studied in the field to statistically analyze the field and satellite data.

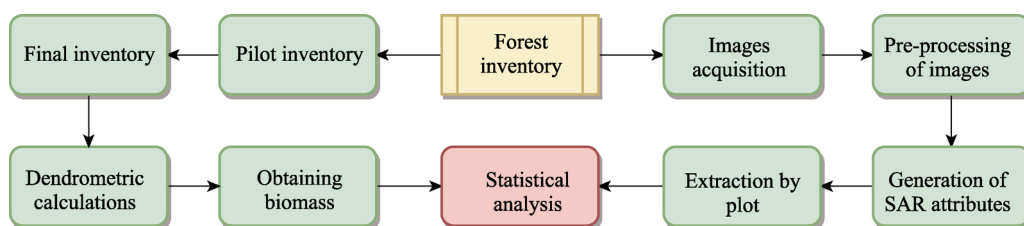


Fig. 2 Methodological flowchart of the study. SAR, synthetic aperture radar.

2.3 Obtaining field data and estimating arboreal aboveground biomass

The fieldwork was conducted in two moments, as indicated in the methodological flowchart (Fig. 2). The pilot inventory was carried out from 16 to 20 December, 2018, and the final inventory was from 8 to 15 September, 2019. Both field data collection methods were chosen considering the Caatinga phenology study by Jesus et al. (2021) to carry out the dendrometric survey in the intermediate phenological condition of the vegetation and, simultaneously, in times close to both the rainy and dry seasons. As there is a high rainfall variation characteristic of the region, it was possible to obtain the AGB data for the intermediate period and associate the AGB with the green and dry periods of the vegetation close to the dates of the inventories.

The choice of areas for implementing these sampling units was based on the variation in the conservation status of the analyzed vegetation (degraded to be conserved) from the interference of human activities. Nineteen plots were installed to carry out the Caatinga inventory, distributed near the Grota do Angico conservation unit (Fig. 1), considering the maximum variation of vegetation concerning biomass, density, composition, and distribution of individuals. Further information can be found in the study of Jesus et al. (2022), which also provides the species' taxonomic identification, classification, and nomenclature. In general, the dominant tree species in the vegetation studied were *Cenostigma pyramidale* (Tul.) Gagnon & G. P. Lewis, with 1240 individuals measured (51.8% of the total), followed by *Aspidosperma pyrifolium* Mart. e Zucc. with 542 representatives, *Jatropha mollissima* (Pohl) Baill. with 150 individuals, *Mimosa tenuiflora* (Willd.) Poir. with 120 individuals, and *Piptadenia retusa* P. G. Ribeiro, Seigler & Ebinger with 109 individuals.

The plot was delimited by an area of 30 m×30 m (900 m²), totaling an inventoried area of 16,200 m². Each one was properly georeferenced by the absolute method using a Garmin GPSMap branded C/A GNSS receiver. Within each sampling unit, we recorded all living and dead individuals from the circumference values at breast height (CBH) (1.3 m from the ground) of the stems equal to or greater than 6.0 cm according to the Caatinga Forest Management Network (2005). Each registered individual had their CBH measured using a measuring tape and their respective total height (H) with a telescopic rod. Subsequently, for each CBH value per individual,

the equivalent diameter (DBH, diameter at breast height) was obtained since it is a dendrometric measure with numerous applications in research in the Caatinga biome (Lima et al., 2018; Lopes et al., 2020; Souza et al., 2020; Menezes et al., 2021; Pereira et al., 2021). Then, the AGB of individual trees was calculated using the allometric equation of Sampaio and Silva (2005): $0.173 \times (\text{DBH})^{2.295}$, $R^2=0.9184$, for all registered individuals. After measuring the biomass (kg) in each plot, it was converted to megagrams per hectare (Mg/hm^2).

2.4 Acquisition, pre-processing, and retrieval of Sentinel-1 data

The acquisition date of the images used estimated the state of the Caatinga leaf cover from the variation of the normalized difference vegetation index (NDVI) values for the study period. For this, the periods of high, intermediate, and low NDVI values were selected, which indicate the green, intermediate, and dry conditions of the vegetation, respectively, considering similar NDVI values for each phenological condition of the Caatinga biome for the years studied (Fig. 3) using Sentinel-1 images acquired on: 2019/01/18–2019/09/03 (yyyy/mm/dd) for the green period, 2018/08/15–2019/10/09 for the intermediate period, and 2018/10/26–2019/11/26 the dry period.

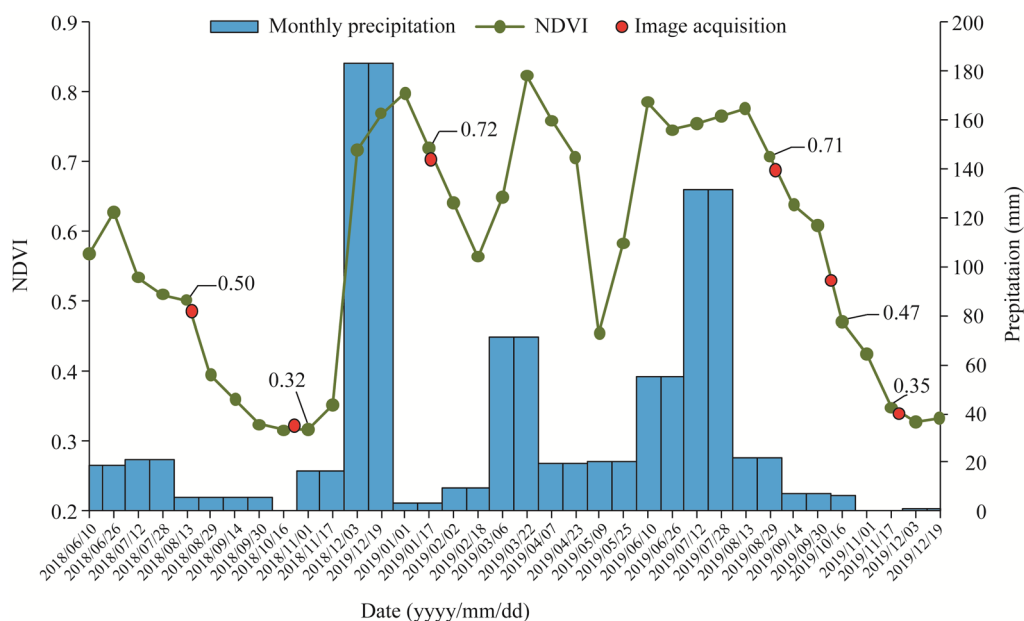


Fig. 3 Distribution of monthly precipitation and NDVI (normalized difference vegetation index), emphasizing NDVI for periods close to Sentinel-1 image acquisition (green: 0.72 and 0.71; intermediate: 0.50 and 0.47; and dry: 0.32 and 0.35).

The NDVI values were obtained with pre-filtering in the dense arboreal Caatinga biome using the temporal vegetation analysis system (SATVeg) web-based tool. The MODIS (moderate-resolution imaging spectroradiometer) NDVI spatial resolution is $250 \text{ m} \times 250 \text{ m}$, and has a temporal resolution of the composition every 16 d (Embrapa, 2018). The monthly precipitation was acquired from the Canindé de São Francisco meteorological station and provided by the Agricultural Development Company of Sergipe on its website (Emdagro, 2020).

Sentinel-1 images of the study plots were acquired directly from the website of the European Space Agency (ESA, 2020a) during the two-year duration of the study. Sentinel-1 images were in descending mode, in orbit 82, interferometric wide mode, which has a swath width of 250 km, incidence angle range of 29.1° – 46.0° , 3 sub-swaths, azimuth steering angle $\pm 0.6^\circ$, and dual and single polarization. Ground range detected (GRD) in high resolution and single look complex (SLC) formats with, respectively, pixel spacing of $10.0 \text{ m} \times 10.0 \text{ m}$ and $2.3 \text{ m} \times 14.1 \text{ m}$, number of

looks 5×1 and 1×1 , an equivalent number of looks 4.4 and 1.0, both level 1, in VV (vertical transmit and vertical receive) and VH (vertical transmit and horizontal receive) polarizations were used.

We pre-processed the GRD images according to Filipponi (2019), so there was a similarity in the pixel dimension of the SLC in relation to the GRD. Multilooking was applied with four looks, 1 in azimuth and 4 in range, and the images were cut (Subset) in both to speed up data processing. The gamma 5×5 filter was selected in the GRD images. In the SLC images, polarimetric filters were applied, which presented results with a more significant relationship with the AGB for each period studied. From the GRD images, VV, VH, and VH/VV polarization data in decibels (dB) were used; the following were also generated: the radar vegetation index (RVI) proposed by Kim and Zyl (2004) and modified for Sentinel-1 by Nasirzadehdizaji et al. (2019), and the dual polarization SAR vegetation index (DPSVI) proposed by Periasamy (2018), both in a linear format. The attributes entropy (H) and alpha angle (α) were obtained in the SLC images. All image processing and extraction of the attributes used (VH, VV, VH/VV, RVI, DPSVI, H, and α) were performed with the Sentinel's application platform (SNAP) v.8.0 tool (ESA, 2020b), sampling each plot in each band using the QGIS (quantum geographic information system) software v.3.18.

2.5 Statistical analysis

The SAR attributes were individually evaluated using simple linear regression, observing the contribution of each in the estimate of AGB in the arboreal Caatinga biome in each evaluated period, analyzing the hypothesis test from the P value analysis of the 5% significance level, and the respective coefficient of determination (R^2) and root mean squared error (RMSE) for the linear equations. Subsequently, multiple linear regressions were calculated considering all possible combinations of the attributes used, selecting the best equation for estimating biomass adopting the principle of parsimony for each period evaluated, considering the R^2 , correlation coefficient (r), and RMSE. The respective graph relationship between the observed and estimated data and the distribution of residual errors was also made. The statistical analysis was performed using the R Core Team 2021 software v.4.1.0.

3 Results

The AGB distribution for each plant individual in all plots showed similar behavior. The largest number of representatives had lower values for the AGB, with small peaks for this variable around 50.00 kg (Fig. 4a). Nevertheless, it appears that this increase varies quantitatively between some plots, such as plots 10, 11, and 18, with the increase in the number of individuals with lower AGB values, and plot 17, with an increase of individuals with a higher AGB value. In addition, we noted that, in general, each plot has individuals who stood out in terms of their biomass; however, we observed that plots 7, 9, 14, 16, and 17 had individuals with much higher AGB values than the tree representatives of the other plots. Plot 14, despite only having one individual, had the individual with the highest biomass (1875.66 kg) in the inventory. The opposite occurred in plot 11, with low AGB values with two arboreal representatives. Plot 11 was still the one that presented the smallest amount of AGB calculated per plot considering those with individuals registered. Plot 19 had no arboreal representative (0.00 kg of AGB). There was also variation in total biomass between the inventoried plots, with plots 10, 18, 12, 8, 17, and 4 presenting AGB between 10.00 and 20.00 Mg/hm², plots 14 and 7 with 20.84 and 21.60 Mg/hm², respectively, and plots 13 and 1 with 32.80 and 39.83 Mg/hm², respectively. Plots 9, 16, 15, 6, 2, 3, and 5 had the higher AGB values, and plot 5 had the highest AGB calculated with 46.63 Mg/hm² (Fig. 4b).

The hypothesis test results through the P value statistical analysis (Table 1) showed that no SAR attribute explained the Y variable (AGB) of each respective simple linear regression equation during the green period. In the other two periods evaluated, we observed that two SAR attributes presented significant differences at the 5% significance level. The VH attribute stood

out in the intermediate and dry periods, with P values of 0.030 and 0.034, respectively. Nevertheless, the lowest P values were observed for α in the intermediate period (0.022) and VV polarization in the dry period (0.010).

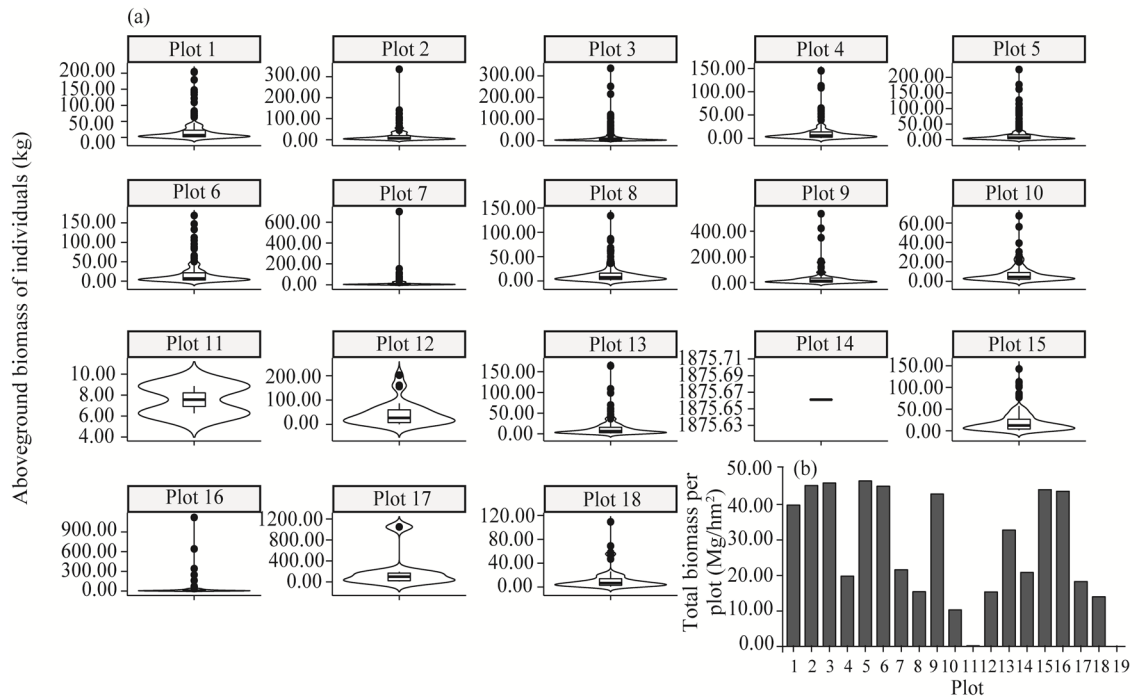


Fig. 4 Distribution of aboveground biomass of individuals (plot 19 had no boxplot because there was no individual, a) and total biomass of each plot (b). In Figure 4a, boxes indicate the IQR (interquartile range, 75th to 25th of the data). The median value is shown as a line within the box. Whiskers extend to the most extreme value within 1.5×IQR. Outlier is shown as circle.

Table 1 Values for the simple linear regression hypothesis test for each SAR (synthetic aperture radar) attribute for each analyzed period

Index	Green period				Intermediate period				Dry period			
	B	SE	t	P value	B	SE	t	P value	B	SE	t	P value
VH	4.97	2.74	1.809	0.088	4.10	1.73	2.366	0.030*	3.73	1.61	2.306	0.034*
VV	3.35	3.19	1.051	0.307	3.71	2.61	1.423	0.172	6.61	2.28	2.896	0.010*
VH/VV	−4.88	19.74	−0.248	0.807	−19.00	23.79	−0.798	0.436	22.03	29.68	0.742	0.468
DPSVI	−13.12	29.03	−0.452	0.657	11.78	26.98	0.437	0.667	−1.00	29.71	−0.034	0.973
RVI	12.95	19.63	0.660	0.518	26.02	17.13	1.518	0.147	21.42	14.52	1.475	0.158
H	46.77	62.40	0.749	0.464	50.02	40.97	1.221	0.239	34.58	41.48	0.834	0.416
α	−0.27	0.95	−0.285	0.779	1.47	0.59	2.500	0.022*	0.81	0.66	1.218	0.240

Note: B, equation coefficients; SE, standard error; t , students t test; P , probability of significance; VH, vertical transmit and horizontal receive; VV, vertical transmit and vertical receive; DPSVI, dual polarization synthetic aperture radar vegetation index; RVI, radar vegetation index; H, attributes entropy; α , alpha angle. The abbreviations are the same as in the following figures and tables. *, $P < 0.05$ level.

When analyzing the quality of adjustment of the SAR attributes individually, a weak relationship of each one in relation to the estimated biomass was observed since low R^2 and high RMSE were verified in all evaluated periods (Fig. 5). The VH polarization was highlighted in relation to the others, presenting the highest R^2 for the green vegetation (0.161), the period that generally presented the lowest values for this coefficient. This attribute stood out and was the second with the values for this coefficient for the intermediate (0.238) and dry (0.248) periods.

The highest R^2 among the three periods was obtained in the polarization VV-dryness (0.330) and α -intermediate (0.269). We also verified that the attributes with the best R^2 had the highest RMSE values, except for α -intermediate, which presented the lowest RMSE value (14.39 Mg/hm²) among the ones analyzed in the three periods.

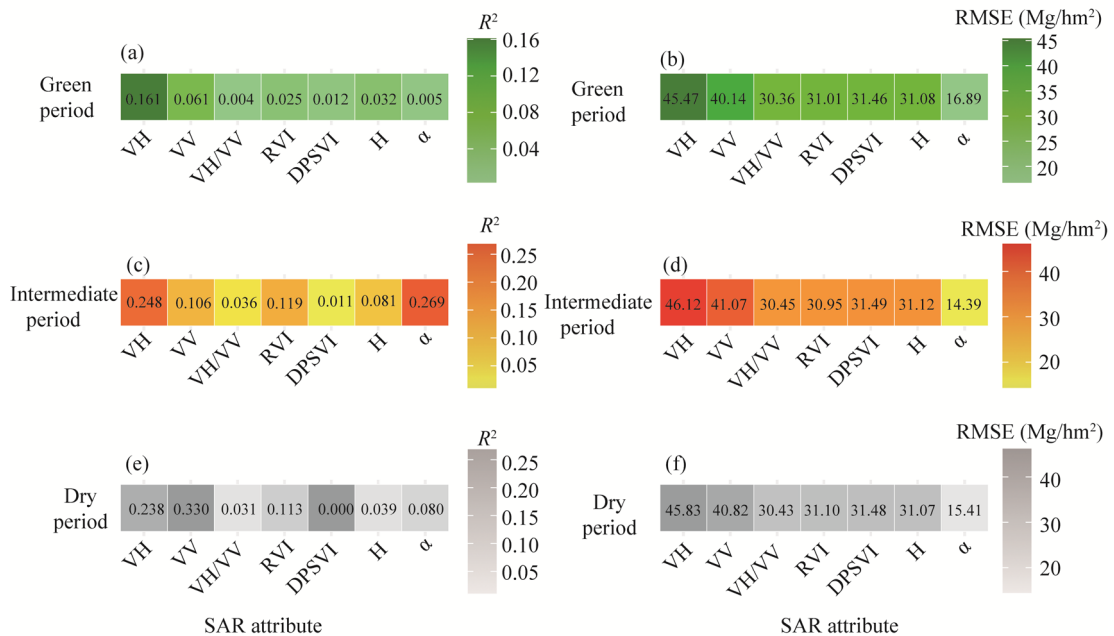


Fig. 5 R^2 (coefficient of determination) and RMSE (root mean squared error) of the analyzed SAR (synthetic aperture radar) attributes for estimating the AGB (aboveground biomass) of arboreal Caatinga biome for each period evaluated. (a and b), green period; (c and d), intermediate period; (e and f), dry period.

When performing the multiple linear regressions, we observed that the DPSVI attribute was present in the composition of the equations in the three periods evaluated (Table 2). In the dry period, the best combination between the attributes was verified only with the DPSVI and cross-polarization (i.e., VH). Additionally, considering the composition by attributes, the equations for the green and intermediate periods differed only between the polarizations VV and VH, respectively, highlighting the importance of the attributes, i.e., VH/VV, H, and α , in addition to the aforementioned vegetation index, in the relationship to estimate the AGB.

Table 2 Multiple linear regression model for estimating the AGB (aboveground biomass) of arboreal Caatinga biome for each period evaluated

Period	Biomass equation	R^2/r	RMSE (Mg/hm ²)
Green	$343.119 + 17.72 \times VV - 115.896 \times VH/VV - 84.557 \times DPSVI + 233.448 \times H - 4.428 \times \alpha$	0.720/0.85	8.40
Intermediate	$342.552 + 9.920 \times VH - 45.972 \times VH/VV - 126.629 \times DPSVI - 129.917 \times H + 2.021 \times \alpha$	0.730/0.85	8.33
Dry	$195.06 + 8.52 \times VH - 102.93 \times DPSVI$	0.550/0.74	10.65

Note: R^2 , coefficient of determination; r , correlation coefficient; RMSE, root mean squared error.

We found that the best equations for estimating AGB generated much higher R^2 values (0.720 for the green period, 0.730 for the intermediate period, and 0.550 for the dry period, respectively) than the simple regressions. Consequently, the multiple linear equations established a high positive correlation between the observed and estimated variables, with r values of 0.85 for the green and intermediate periods and 0.74 for the dry period. Although the relationship between the observed and estimated AGB variables of the multiple regression during the intermediate period was the only one that presented an estimate of 50.00 Mg/hm² (plot 5), we observed that the data are distributed closer to the straight line of the equation obtained when compared with the green

and dry periods (Fig. 6).

Residual analysis by RMSE (Table 2) showed that the AGB estimation equation for the intermediate period (8.33 Mg/hm^2) was lower than the green (8.40 Mg/hm^2) and dry (10.65 Mg/hm^2) periods. When observing the distribution of the residual error by sample plot (Fig. 6), it was verified that the variation of the scale of the residue followed the same increasing order of the RMSE, with an amplitude of 28.20 Mg/hm^2 for the intermediate period, 30.50 Mg/hm^2 for the green and 39.57 Mg/hm^2 for the dry period. Plots 4, 15 and 16 are among the ones that showed more discrepancies between the estimated and observed AGB, also highlighting the plot 9 for the green and dry periods, and additionally plot 11 for the dry period.

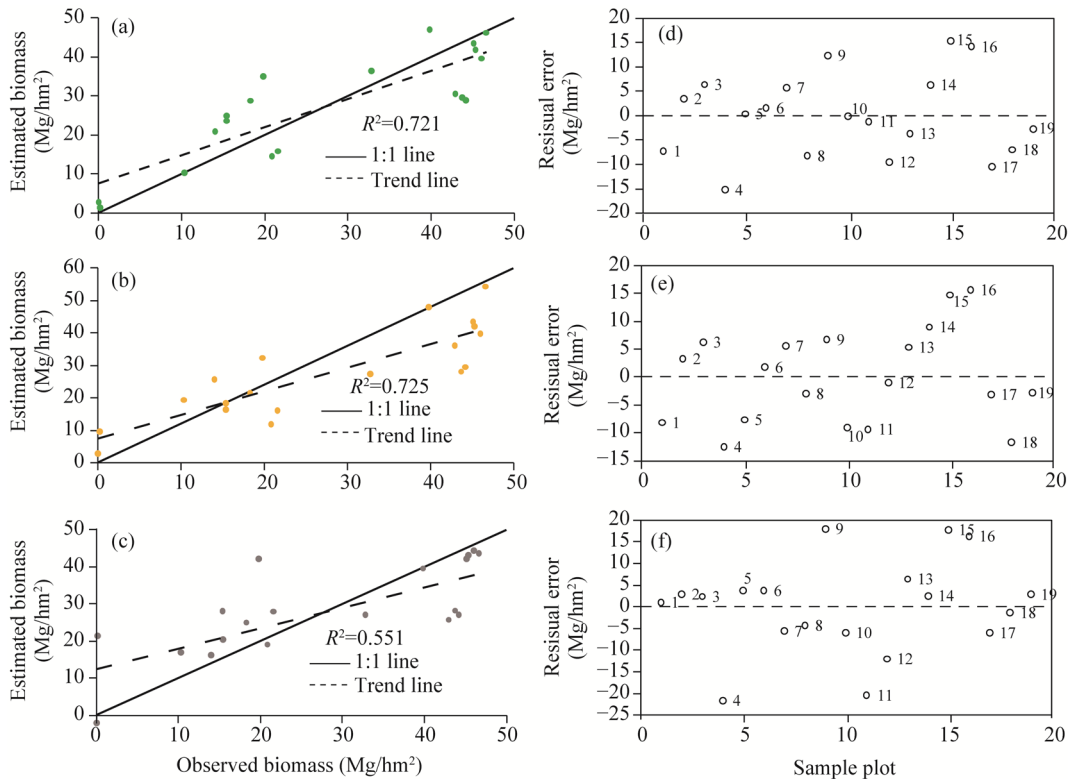


Fig. 6 Relationship between the observed AGB (aboveground biomass) and the estimated AGB by best multiple linear regression model (a, green period; b, intermediate period; c, dry period) and their respective residuals per sample plot for each analyzed value (d–f)

4 Discussion

The calculated AGB showed that the vast majority of arboreal individuals have low values for this variable in the Caatinga biome of the studied area, indicating that there is a high number of individuals with smaller dendrometric dimensions, mainly diameters, which is a characteristic of forest communities in regeneration and also verified in other inventories in this biome (Lima et al., 2018; Lopes et al., 2020; Nascimento Neto et al., 2020). The influence of the diameter on the AGB in the measured arboreal individuals caused the different biomass responses of the Caatinga biome in the inventoried plots. This was verified when comparing plots 11 and 14, which had 2 and 1 individuals, respectively, but totally differed in the AGB, presenting 0.17 and 20.84 Mg/hm^2 , respectively. This influence was also verified in the variation of AGB in relation to the number of individuals in the other plots, with plots 7, 8, 9, 7, 11, and 17 having fewer individuals, not being among the ones with the lowest calculated biomass, indicating the variability of the composition of the sampling units used. Despite this, the plots with the highest number of tree representatives (2, 3, 5, 6, and 15) had the highest AGB, except for plot 13, with 228 measured individuals but

32.80 Mg/hm², as a result of their small diameters. Therefore, the variation of the AGB is also a result of the different vegetation phytophysiognomies and conservation status of the sample units in this biome, as also verified by Castanho et al. (2020b) and Menezes et al. (2021).

Regarding the statistical relationship by linear regression of the AGB per plot and each SAR attribute analyzed, we observed that there is slight variation in the responses since the vast majority of interactions for the phenological periods evaluated had no significant difference at the 5% level of significance, showing that the attributes individually do not influence the AGB. Nevertheless, it was noted that four responses had an impact on the AGB equation, with emphasis on the VH polarization being the only statistically significant attribute in two periods (intermediate and dry). This shows variation between the responses of some SAR attributes and the phenological period of the vegetation and that the AGB estimates depend on the image acquisition station (Nguyen et al., 2016). However, despite these interactions impacting this estimate, there was little relationship between all SAR attributes and the AGB, as evidenced by the low R^2 and high RMSE values.

Among the polarized data, the VH attribute even presented the highest R^2 for the green period (0.161), being the second most accurate for the intermediate (0.248) and dry (0.238) periods, showing the importance of the interaction of this polarization in the three seasonalities of the Caatinga biome. However, the VV polarization stood out with the highest R^2 (0.330) in the dry period, among the other attributes and periods, indicating a greater response to the interaction of this polarized data with the vegetation without leaves, possibly indicating that the backscatter intensity of this polarization was more sensitive to the AGB in the dry season than in the rainy season (Nguyen et al., 2016). Malhi et al. (2021) also found that the VV polarization was superior in accuracy ($r=0.74$) compared with the cross-polarization ($r=0.05$) of Sentinel-1 when analyzing the AGB of the dense tropical forest in the Shoolpaneshwar Wildlife Sanctuary in Gujarat, India. Nonetheless, different results were seen by Navarro et al. (2019) with R^2 of 0.900 in a mangrove forest of Senegal with the AGB below 35.00 Mg/hm²; Safari and Sohrabi (2020) found a better correlation with the AGB in retrieval in Zagros oak forests in the Kermanshah Province (western Iran) and by Nuthammachot et al. (2022), who indicated that cross-polarization may be more sensitive to the AGB than co-polarization.

The contribution of VH polarization in estimating AGB as seen in the green and intermediate periods compared with VV and HH may be due to the lower influence of soil moisture on its response (Huang et al., 2018). Furthermore, this attribute is associated with a greater volumetric dispersion caused by the high canopy density (Laurin et al., 2018). This polarization was also important in the composition of the multiple linear equations in the intermediate and dry periods, which may be related to its interaction with the high number of ramifications characteristic of the analyzed Caatinga biome, consequently, resulting in more significant volumetric scattering, which is expected by cross-polarization.

Comparing the accuracy of the present study with others that used data obtained from Sentinel-1 to estimate the AGB in drylands (Table 3), we observed that only the study of Forkuor et al. (2020) in the African savanna presented R^2 (0.760) above those reported herein (0.730), even using only the backscatter coefficients. David et al. (2022), also in the African savanna and using the backscatter coefficients, obtained a lower R^2 (0.580), demonstrating the variation of radar responses regarding the AGB estimate. Variation in the accuracy of this estimate was also observed by Jesus et al. (2023) in the same arboreal Caatinga biome of this study using data from H and α , showing that only these types of information do not provide good accuracy (0.320) in the relationship between the associated variables. Studies in other dry environments also showed lower R^2 values, as performed by Bao et al. (2019), who used backscatter coefficients together with texture data, verifying the best accuracy (0.500) of the VH polarization in estimating the AGB of the Hulun Buir grassland in China, and Pötzschner et al. (2022) who verified an R^2 of 0.690 using backscatter coefficients in the vegetation of the dry Chaco ecoregion in South America.

Cross-polarization was also highlighted in studies using the L band, such as the one by

Table 3 Examples of the AGB estimation in drylands using the Sentinel-1 SAR (synthetic aperture radar) data

Reference	Type of forest, location	SAR attribute	R^2
Present study	Caatinga, Brazil	Coherent and incoherent	0.730
Jesus et al. (2023)	Caatinga, Brazil	H and α	0.320
David et al. (2022)	Savanna, Southern Africa	Backscatter coefficients	0.580
Forkuor et al. (2020)	Sudanian savanna, West Africa	Backscatter coefficients	0.760
Bao et al. (2019)	Hulun Buir grassland, China	Backscatter coefficients and texture	0.500
Pötzschner et al. (2022)	Dry Chaco ecoregion, South America	Backscatter coefficients	0.690

Mitchard et al. (2009), who verified the better performance of HV polarization ($R^2=0.730$) compared to HH ($R^2=0.550$) of ALOS PALSAR (advanced land observing satellite phased array L-band synthetic aperture radar) images in different vegetation formations including savanna regions in Cameroon, Uganda, and Mozambique in Africa. Moreover, Nguyen et al. (2016), with data from ALOS PALSAR-2, found that HV polarization could explain the 54% variation in biomass in a tropical forest with deciduous characteristics in Vietnam. Wingate et al. (2018) found an accuracy of $R^2=0.740$ in estimating the AGB of the savanna in northeastern Namibia using data from PALSAR and PALSAR-2 from linear logarithmic models. Braun et al. (2018) estimated the AGB in low-biomass savanna ecosystems and obtained as the best response an R^2 value of 0.520 using the combination of data from ALOS PALSAR, Envisat (environmental satellite), and special sensor microwave/imager (SSM/I) with nonlinear regression, indicating the use of the exponential model to adjust the data distribution. However, they also pointed out that other statistical techniques, such as linear, logarithmic, or multivariate, could present good results, depending on the relationship between the AGB and radar backscatter.

This was verified by analyzing the response in dry period, which, when associating the VH polarization with the DPSVI, presented an R^2 (0.550) higher than all the responses of the attributes individually at all times. However, despite the increase in this relationship in this period, adding the other attributes did not increase the accuracy for estimating AGB. The same was reported by Forkuor et al. (2020) when estimating the AGB in the savanna, in which the largest number of SAR variables (VV, VH, VH-VV, and VH+VV) of Sentinel-1 in the model did not provide improvement in accuracy ($R^2=0.660$), with a better estimate being verified when using only the VH and VV polarizations ($R^2=0.760$). Regarding the green and intermediate periods, there was a significant increase in accuracy when using five attributes that had a relationship and impact on the estimation of the AGB, with high R^2 and low RMSE.

Among the attributes used in the multiple linear regression to estimate the AGB of the arboreal Caatinga biome, the DPSVI stood out, being present in the estimation models in the three periods analyzed. Periasamy (2018) also found that the DPSVI was relevant in estimating the AGB in the Perambalur District in Tamil Nadu, India, with landscapes composed of forest and barren land areas, both in the dry ($R^2=0.730$) and rainy seasons ($R^2=0.700$) through simple linear regression, which showed that this index was related to the biomass of the analyzed vegetation.

The band ratio composed the multiple linear equations in the green and intermediate periods, differing from the result reported by Laurin et al. (2018), who observed a more significant relation of this attribute of Sentinel-1 under deciduous vegetation conditions. The band ratio could be sensitive to interaction of SAR data with small branches, which are more exposed when there is no canopy, contributing to AGB given a large number of branches. Nevertheless, this difference can be explained because the area in their study comprises broadleaf forests and high AGB, the opposite of the Caatinga physiognomy.

The coherent attributes (H and α) of the Sentinel-1 images were also relevant in estimating the AGB of the Caatinga biome in the green and intermediate periods. The result indicates that information about the type of scattering and its randomness from microwave phase data contributes to the multiple relationships with the estimated variable, which would not be possible

to have in the incoherent data from the backscatter coefficients. Cartus et al. (2021) studied semi-arid forest areas in the Sierra National Forest in California, USA, and Ghosh and Behera (2021) also verified its importance in modeling from the AGB estimate in India's eastern coast tropical mangrove forests, despite using other coherent Sentinel-1 data. The same was evidenced by Huang et al. (2018) using information obtained from the polarimetric decomposition of the L-band of PALSAR-2, such as the alpha angle, generating more accurate AGB estimation models in the eastern temperate forest in northern New England, USA.

Despite the good relationship between the observed and estimated AGB obtained in the present study, it is important to note that in the analyzed Caatinga biome, there are other components present in the sample plots, such as herbaceous plants (*Croton heliotropiifolius* Kunth, *Helleborus foetidus* L., *Senna obtusifolia* (L.) H.S.Irwin & Barneby), Cactaceae such as *Cereus jamacaru* DC. and *Xiquexique gounellei* (F.A.C.Weber) Lavor & Calvente, and even exposed stones as is characteristic of the region's soil, which may have caused errors in the estimate. Therefore, the presence of these elements may have influenced the interaction of the radar signal since the microwave interacts with all components of the plot resulting in Sentinel-1 image pixels affected by components that are not just the AGB of the estimated vegetation.

5 Conclusions

This study found that combining polarized attributes with those from the polarimetric decomposition of Sentinel-1 images allowed a high correlation with the AGB estimate of the studied arboreal Caatinga biome using multiple linear regression. The use of isolated attributes, however, did not generate a good relationship between the estimated and observed variable for the evaluated vegetation conditions. The phenological condition of the Caatinga biome with the best result regarding the biomass estimate was the intermediate period, followed by the green period, with only the difference of the VH attribute by the VV, respectively, in the composition of the multiple linear equations. Despite the vegetation under strong drought (dry period) presenting the lowest R^2 among the multiple regressions, its value was superior to all attributes when used individually in the three conditions of the Caatinga biome.

Therefore, Sentinel-1 C-band images can be used to estimate the AGB of the arboreal Caatinga biome as it presented a high correlation between its attributes with the estimated variable. In addition, Sentinel-1 is an alternative to optical images, considering the difficulty of obtaining images without clouds. However, although this study seeks as much variation as possible in the local vegetation, it is noteworthy that the Caatinga biome has different phytophysiognomies, and it is necessary to observe the capacity of estimating the AGB in each typology, as well as the allometric equation that best estimates the vegetation biomass. Likewise, different pre-processing in the images and using other data obtained from this radar can generate other results in correlations for estimating AGB.

Acknowledgements

The authors thank the National Council for Scientific and Technological Development (CNPq) and the Coordination of Superior Level Staff Improvement, Brazil (CAPES) for supporting this research.

References

- Akhtar A M, Qazi W A, Ahmad S R, et al. 2020. Integration of high-resolution optical and SAR satellite remote sensing datasets for aboveground biomass estimation in subtropical pine forest, Pakistan. *Environmental Monitoring and Assessment*, 192: 584.
- Althoff T D, Menezes R S C, Carvalho A L, et al. 2016. Climate change impacts on the sustainability of the firewood harvest and vegetation and soil carbon stocks in a tropical dry forest in Santa Teresinha Municipality, Northeast Brazil. *Forest Ecology and Management*, 360: 367–375.
- Alvares C A, Stape J L, Sentelhas P C, et al. 2014. Köppen's climate classification map for Brazil. *Meteorologische Zeitschrift*,

- 22(6): 711–728.
- Baccini A, Friedl M A, Woodcock C E, et al. 2004. Forest biomass estimation over regional scales using multisource data. *Geophysical Research Letters*, 31(10): L10501, doi: 10.1029/2004GL019782.
- Baccini A, Goetz S J, Walker W S, et al. 2012. Estimated carbon dioxide emissions from tropical deforestation improved by carbon-density maps. *Nature Climate Change*, 2: 182–185.
- Bao N, Li W, Gu X, et al. 2019. Biomass estimation for semiarid vegetation and mine rehabilitation using Worldview-3 and Sentinel-1 SAR imagery. *Remote Sensing*, 11(23): 2855, doi: 10.3390/rs11232855.
- Barbosa Neto M V B, Araújo M S B, Araújo Filho J C, et al. 2021. Rill and sheet soil erosion estimation in an area undergoing desertification in the Brazilian semi-arid region. *Modeling Earth Systems and Environment*, 7: 1183–1191.
- Bastin J F, Berrahmouni N, Grainger A, et al. 2017. The extent of forest in dryland biomes. *Science*, 356(6338): 635–638.
- Bezerra F G S, Aguiar A P D, Alvalá R C S, et al. 2020. Analysis of areas undergoing desertification, using EVI2 multi-temporal data based on MODIS imagery as indicator. *Ecological Indicators*, 117: 106579, doi: 10.1016/j.ecolind.2020.106579.
- Braun A, Wagner J, Hochschild V. 2018. Above-ground biomass estimates based on active and passive microwave sensor imagery in low-biomass savanna ecosystems. *Journal of Applied Remote Sensing*, 12(4): 046027, doi: 10.1117/1.JRS.12.046027.
- Cartus O, Santoro M, Wegmüller U, et al. 2021. Sentinel-1 coherence for mapping above-ground biomass in semiarid forest areas. *IEEE Geoscience and Remote Sensing Letters*, 19: 4012805, doi: 10.1109/LGRS.2021.4012805.
- Castanho A D A, Coe M T, Brando P, et al. 2020a. Potential shifts in the aboveground biomass and physiognomy of a seasonally dry tropical forest in a changing climate. *Environmental Research Letters*, 15(3): 034053, doi: 10.1088/1748-9326/ab7394.
- Castanho A D A, Coe M T, Andrade E M, et al. 2020b. A close look at above ground biomass of a large and heterogeneous seasonally dry tropical forest—Caatinga in North East of Brazil. *Annals of the Brazilian Academy of Sciences*, 92(1): e20190282, doi: 10.1590/0001-3765202020190282.
- David R M, Rosser N J, Donoghue D N M. 2022. Improving above ground biomass estimates of Southern Africa dryland forests by combining Sentinel-1 SAR and Sentinel-2 multispectral imagery. *Remote Sensing of Environment*, 282: 113232, doi: 10.1016/j.rse.2022.113232.
- Embrapa (Brazilian Agricultural Research Corporation). 2011. Brazilian system of soil classification. Brazilian soils. Soil map of Brazil. [2021-01-11]. <https://www.embrapa.br/tema-solos-brasileiros/solos-do-brasil>. (in Portuguese)
- Embrapa (Brazilian Agricultural Research Corporation). 2018. SATVeg. Vegetation Temporal Analysis System. [2021-01-10]. <https://www.satvegcnptiaembrapa.br/satveg/loginhtml>. (in Portuguese)
- Emdagro. 2020. Agricultural Development Company of Sergipe. Statistic Agriculture. Rainfall. [2021-01-10]. <https://www.emdagrosegovbr/pluviosidade/>. (in Portuguese)
- ESA (European Space Agency). 2020a. Copernicus. Open Access Hub. [2021-10-14]. <https://scihubcopernicuseu/dhus/#/home>.
- ESA (European Space Agency). 2020b. SNAP. [2021-11-18]. <https://stepesaint/main/download/snap-download/>.
- FAO (Food and Agriculture Organization of the United Nations). 2012. Global Ecological Zones for FAO Forest Reporting: 2010 Update. Rome: Forest Resources Assessment Working, 52.
- Fernandes M R M. 2018. Estimation of basal area, volume and biomass in a fragment of Caatinga dense hyperxerophile in the high Sergipe sertão based on data MSI/Sentinel-2. PhD Dissertation. Espírito Santo: Federal University of Espírito Santo. (in Portuguese)
- Filipponi F. 2019. Sentinel-1 GRD preprocessing workflow. *Proceedings*, 18(1): 11, doi: 10.3390/ECRS-3-06201.
- Forkuor G, Zoungrana J-B B, Dimobe K, et al. 2020. Above-ground biomass mapping in West African dryland forest using Sentinel-1 and 2 datasets—A case study. *Remote Sensing of Environment*, 236: 111496, doi: 10.1016/j.rse.2019.111496.
- Ghosh S M, Behera M D. 2021. Aboveground biomass estimates of tropical mangrove forest using Sentinel-1 SAR coherence data—the superiority of deep learning over a semi-empirical model. *Computers & Geosciences*, 150: 104737, doi: 10.1016/j.cageo.2021.104737.
- Huang X, Ziniti B, Torbick N, et al. 2018. Assessment of forest above ground biomass estimation using multi-temporal C-band Sentinel-1 and polarimetric L-band PALSAR-2 data. *Remote Sensing*, 10(9): 1424, doi: 10.3390/rs10091424.
- INSA (Semi Arid National Institute). 2019. Global Network of Dryland Research Institute. [2021-03-22]. <https://www.gndri.org/institutions/semi-arid-national-institute-instituto-nacional-do-semiarido-insa/>. (in Portuguese)
- Jesus J B, Souza B B, Oliveira A M S, et al. 2019a. Aridity index and climatic risk of desertification in the semi-arid state of Sergipe. *Brazilian Journal of Climatology*, 24: 214–227.
- Jesus J B, Ribeiro M M, Kuplich T M, et al. 2019b. Statistical analysis of the spatial relationship of Caatinga and physiographic factors through remote data. *Revista Floresta*, 49(4): 755–762.
- Jesus J B, Kuplich T M, Barreto I D C, et al. 2021. Temporal and phenological profiles of open and dense Caatinga using

- remote sensing: Response to precipitation and its irregularities. *Journal of Forestry Research*, 32: 1067–1076.
- Jesus J B, Oliveira D G, Araújo W S, et al. 2022. Influence of anthropization on the floristic composition and phytosociology of the Caatinga susceptible to desertification in the state of Sergipe, Brazil. *Tropical Ecology*, 63: 398–408.
- Jesus J B, Kuplich T M, Barreto I D C, et al. 2023. Dual polarimetric decomposition in Sentinel-1 images to estimate aboveground biomass of arboreal caatinga. *Remote Sensing Applications: Society and Environment*, 29: 100897, doi: 10.1016/j.rsase.2022.100897.
- Kim Y, van Zyl J. 2004. Vegetation effects on soil moisture estimation. In: *Proceedings of the International Geoscience and Remote Sensing Symposium. IEEE International Geoscience and Remote Sensing Symposium*, Anchorage: Institute of Electrical and Electronics Engineers, 800–802.
- Kumar L, Sinha P, Taylor S, et al. 2015. Review of the use of remote sensing for biomass estimation to support renewable energy generation. *Journal of Applied Remote Sensing*, 9(1): 097696, doi: 10.1117/1.JRS.9.097696.
- Laurin G V, Balling J, Corona P, et al. 2018. Above-ground biomass prediction by Sentinel-1 multitemporal data in central Italy with integration of ALOS2 and Sentinel-2 data. *Journal of Applied Remote Sensing*, 12(1): 016008, doi: 10.1117/1.JRS.12.016008.
- Lima Júnior C, Accioly L J O, Giongo V, et al. 2014. Estimation of "Caatinga" woody biomass using allometric equations and vegetation index. *Scientia Forestalis*, 42(102): 289–298. (in Portuguese)
- Lima R B, Ferreira R L C, Silva J A A, et al. 2018. Diameter structure in a community of shrub-tree Caatinga, municipality of Floresta, state of Pernambuco, Brazil. *Revista Floresta*, 48(1): 133–142.
- Lopes J F B, Andrade E M, Pereira E C B, et al. 2020. Cut cycles and soil carbon potential stocks in a managed forest in the Caatinga domain in Brazil. *Revista Caatinga*, 33(3): 735–745.
- Maia V A, Souza C R, Aguiar-Campos N, et al. 2020. Interactions between climate and soil shape tree community assembly and above-ground woody biomass of tropical dry forests. *Forest Ecology and Management*, 474: 118348, doi: 10.1016/j.foreco.2020.118348.
- Malhi R K M, Anand A, Srivastava P K, et al. 2021. Synergistic evaluation of Sentinel 1 and 2 for biomass estimation in a tropical forest of India. *Advances in Space Research*, 69(4): 1752–1767.
- Mayamanikandan T, Reddy S, Fararoda R, et al. 2020. Quantifying the influence of plot-level uncertainty in above ground biomass up scaling using remote sensing data in central Indian dry deciduous forest. *Geocarto International*, 37(12): 3489–3503.
- Menezes R S C, Sales A T, Primo D C, et al. 2021. Soil and vegetation carbon stocks after land-use changes in a seasonally dry tropical forest. *Geoderma*, 390: 114943, doi: 10.1016/j.geoderma.2021.114943.
- Mitchard E A T, Saatchi S S, Woodhouse I H, et al. 2009. Using satellite radar backscatter to predict above-ground woody biomass: A consistent relationship across four different African landscapes. *Geophysical Research Letters*, 36(23): L23401, doi: 10.1029/2009GL040692.
- MMA (Ministry of the Environment). 2018. Sergipe National Forest Inventory: Main Results. Brasília: Brazilian Forest Service, 87. (in Portuguese)
- MMA (Ministry of the Environment). 2021. Caatinga Biomes. [2021-06-03]. <https://antigommagovbr/biomas/caatingahtml>. (in Portuguese)
- Nascimento Neto J H, Holanda A C, Abreu J C. 2020. Assessing the feasibility of the BDQ method for the sustainable management of the Caatinga. *Revista Caatinga*, 33(3): 746–756.
- Nasirzadehdizaji R, Sanli F B, Abdikan S, et al. 2019. Sensitivity analysis of multi-temporal Sentinel-1 SAR parameters to crop height and canopy Coverage. *Applied Sciences*, 9(4): 655, doi: 10.3390/app9040655.
- Navarro J A, Algeet N, Fernández-Landa A, et al. 2019. Integration of UAV, Sentinel-1, and Sentinel-2 data for mangrove plantation aboveground biomass monitoring in Senegal. *Remote Sensing*, 11(1): 77, doi: 10.3390/rs11010077.
- Nguyen L V, Tateishi R, Nguyen H T, et al. 2016. Estimation of tropical forest structural characteristics using ALOS-2 SAR data. *Advances in Remote Sensing*, 5(2): 131–144.
- Nóbrega R S, Santiago G A C F, Soares D B. 2016. Trends in oceanic climate control under temporal variability of precipitation in Northeast Brazil. *Brazilian Journal of Climatology*, 18: 276–292. (in Portuguese)
- Nuthammachot N, Askar A, Stratoulas D, et al. 2022. Combined use of Sentinel-1 and Sentinel-2 data for improving above-ground biomass estimation. *Geocarto International*, 37(2): 366–376.
- Oliveira C P, Ferreira R L C, Silva J A A, et al. 2021. Modeling and spatialization of biomass and carbon stock using LiDAR metrics in tropical dry forest, Brazil. *Forests*, 12(4): 473, doi: 10.3390/f12040473.
- Oliveira C P, Ferreira R L C, Silva J A A, et al. 2022. Prediction of biomass in dry tropical forests: An approach on the importance of total height in the development of local and pan-tropical models. *Journal of Sustainable Forestry*, 41(10):

983–998.

- Pereira J E S, Barreto-Garcia P A B, Paula A, et al. 2021. Form quotient in estimating Caatinga tree volume. *Journal of Sustainable Forestry*, 40(5): 508–517.
- Periasamy S. 2018. Significance of dual polarimetric synthetic aperture radar in biomass retrieval: An attempt on Sentinel-1. *Remote Sensing of Environment*, 217: 537–549.
- Pötzschner F, Baumann M, Gasparri N I, et al. 2022. Ecoregion-wide, multi-sensor biomass mapping highlights a major underestimation of dry forests carbon stocks. *Remote Sensing of Environment*, 269: 112849, doi: 10.1016/j.rse.2021.112849.
- R Core Team. 2021. R: A language and environment for statistical computing. Version 4.1.0. R Foundation for Statistical Computing, Vienna, Austria.
- Ribeiro A S, Mello A A. 2007. Biota diagnosis. In: Ribeiro A S. *Studies for the Creation of the Grota do Angico Natural Monument*. Sergipe: Secretary of State for the Environment and Water Resources, 12–20. (in Portuguese)
- Saatchi S S, Harris N L, Brown S, et al. 2011. Benchmark map of forest carbon stocks in tropical regions across three continents. *Proceedings of the National Academy of Sciences*, 108(24): 9899–9904.
- Safari A, Sohrabi H. 2020. Integration of synthetic aperture radar and multispectral data for aboveground biomass retrieval in Zagros oak forests, Iran: An attempt on Sentinel imagery. *International Journal of Remote Sensing*, 41(20): 8069–8095.
- Salvatierra L H A, Ladle R J, Barbosa H, et al. 2017. Protected areas buffer the Brazilian semi-arid biome from climate change. *Biotropica*, 49(5): 753–760.
- Sampaio E V S B, Silva G C. 2005. Biomass equations for Brazilian semiarid Caatinga plants. *Acta Botanica Brasilica*, 19(4): 935–943.
- SEMARH (Secretary of State for the Environment and Water Resources). 2012. Digital Atlas about Water Resources in Sergipe. Sergipe: Sergipe Water Resources Information System, 1–3. (in Portuguese)
- Silveira E M O, Terra M C N S, Acerbi-Júnior F W, et al. 2020. Estimating aboveground biomass loss from deforestation in the Savanna and semi-arid biomes of Brazil between 2007 and 2017. In: Suratman M N, Latif Z A, Brunsell N. *Forest Degradation around the World*. London: IntechOpen, 1–17.
- Sörensen L. 2007. A spatial analysis approach to the global delineation of dryland areas of relevance to the CBD. In: *Programme of Work on Dry and Sub-Humid Lands*. Cambridge: UNEP World Conservation Monitoring Centre, 1–8.
- Souza D G, Sfair J C, Paula A S, et al. 2019. Multiple drivers of aboveground biomass in a human-modified landscape of the Caatinga dry forest. *Forest Ecology and Management*, 435: 57–65.
- Souza M T P, Azevedo G B, Azevedo G T O S, et al. 2020. Growth of native forest species in a mixed stand in the Brazilian Savanna. *Forest Ecology and Management*, 462: 118011, doi: 10.1016/j.foreco.2020.118011.
- Tomasella J, Vieira R M S P, Barbosa A A, et al. 2018. Desertification trends in the Northeast of Brazil over the period 2000–2016. *International Journal of Applied Earth Observation and Geoinformation*, 73: 197–206.
- Vaghela B, Chirakkal S, Putrevu D, et al. 2021. Modelling above ground biomass of Indian mangrove forest using dual-pol SAR data. *Remote Sensing Applications: Society and Environment*, 21: 100457, doi: 10.1016/j.rsase.2020.100457.
- Veloso H P, Rangel-Filho A L R, Lima J C A. 1991. Classification of Brazilian vegetation adapted to a universal system. Rio de Janeiro: IBGE, 123. (in Portuguese)
- Vendruscolo J, Marin A M P, Felix E S, et al. 2020. Monitoring desertification in semiarid Brazil: Using the Desertification Degree Index (DDI). *Land Degradation & Development*, 32(2): 684–698.
- Vieira R M S P, Tomasella J, Alvalá R C S, et al. 2015. Identifying areas susceptible to desertification in the Brazilian northeast. *Solid Earth*, 6: 347–360.
- Vieira R M S P, Sestini M F, Tomasella J, et al. 2020. Characterizing spatio-temporal patterns of social vulnerability to droughts, degradation and desertification in the Brazilian northeast. *Environmental and Sustainability Indicators*, 5: 100016, doi: 10.1016/j.indic.2019.100016.
- Vieira R M S P, Tomasella J, Barbosa A A, et al. 2021. Desertification risk assessment in Northeast Brazil: Current trends and future scenarios. *Land Degradation & Development*, 31(1): 224–240.
- Wingate V R, Phinn S R, Kuhn N, et al. 2018. Estimating aboveground woody biomass change in Kalahari woodland: Combining field, radar, and optical data sets. *International Journal of Remote Sensing*, 39(2): 577–606.